



TITLE:

Experimental insights on the electron transfer and energy transfer processes between $\text{Ce}^3\text{-Yb}^3$ and $\text{Ce}^3\text{-Tb}^3$ in borate glass

AUTHOR(S):

Sontakke, Atul D.; Ueda, Jumpei; Katayama, Yumiko; Dorenbos, Pieter; Tanabe, Setsuhisa

CITATION:

Sontakke, Atul D. ...[et al]. Experimental insights on the electron transfer and energy transfer processes between $\text{Ce}^3\text{-Yb}^3$ and $\text{Ce}^3\text{-Tb}^3$ in borate glass. Applied Physics Letters 2015, 106(13): 131906.

ISSUE DATE:

2015-03-30

URL:

<http://hdl.handle.net/2433/231985>

RIGHT:

© 2015 AIP Publishing LLC. The following article appeared in [Appl. Phys. Lett. 106, 131906 (2015); <https://doi.org/10.1063/1.4916946>] and may be found at <https://aip.scitation.org/doi/abs/10.1063/1.4916946>; The full-text file will be made open to the public on 30 March 2016 in accordance with publisher's 'Terms and Conditions for Self-Archiving'.

Experimental insights on the electron transfer and energy transfer processes between Ce^{3+} - Yb^{3+} and Ce^{3+} - Tb^{3+} in borate glass

Atul D. Sontakke,^{1,a)} Jumpei Ueda,^{1,2} Yumiko Katayama,¹ Pieter Dorenbos,² and Setsuhisa Tanabe¹

¹Graduate School of Human and Environmental Studies, Kyoto University, Kyoto 606-8501, Japan

²Delft University of Technology, Faculty of Applied Science, Department of Radiation Science and Technology (FAME-LMR), 2629 JB Delft, The Netherlands

(Received 28 January 2015; accepted 25 March 2015; published online 2 April 2015)

A facile method to describe the electron transfer and energy transfer processes among lanthanide ions is presented based on the temperature dependent donor luminescence decay kinetics. The electron transfer process in Ce^{3+} - Yb^{3+} exhibits a steady rise with temperature, whereas the Ce^{3+} - Tb^{3+} energy transfer remains nearly unaffected. This feature has been investigated using the rate equation modeling and a methodology for the quantitative estimation of interaction parameters is presented. Moreover, the overall consequences of electron transfer and energy transfer process on donor-acceptor luminescence behavior, quantum efficiency, and donor luminescence decay kinetics are discussed in borate glass host. The results in this study propose a straight forward approach to distinguish the electron transfer and energy transfer processes between lanthanide ions in dielectric hosts, which is highly advantageous in view of the recent developments on lanthanide doped materials for spectral conversion, persistent luminescence, and related applications. © 2015 AIP Publishing LLC. [<http://dx.doi.org/10.1063/1.4916946>]

In the past some years, several reports have been published on ultra-violet to visible and visible to near infrared spectral down-conversion in rare earth lanthanides doped glasses and crystals.¹⁻⁵ The spectral down conversion or quantum cutting is a cooperative energy transfer process, where one high energy photon splits into two or more low energy photons. Such processes can significantly increase the photon density at required spectral region and therefore are advantageous for improved lightings and in the solar energy concentration.^{4,5} However, given the cooperative nature of the process and small oscillator strengths of f-f electronic transitions, the external quantum efficiency remains very low.⁵⁻⁷ In this regard, the ongoing claims of observing an efficient quantum cutting especially in the case of $\text{Ce}^{3+}/\text{Eu}^{2+}$ - Yb^{3+} codoped materials raises serious concerns and confusion.⁸⁻¹¹ Recent studies on Ce^{3+} (donor)- Yb^{3+} (acceptor) and other similar redox ions codoped materials have demonstrated that the donor de-excitation and donor to acceptor energy sensitization involves an electron transfer process and not the cooperative energy transfer process as was considered earlier.¹²⁻¹⁵

Electron transfer and energy transfer interactions are well established processes responsible for several physical phenomena such as the energy storage, scintillation, afterglow, quenching, and sensitization.^{16,17} In case of electron transfer, an electron undergoes a physical displacement from one ion or molecule to the other. On the contrary, energy transfer usually takes place through the non-radiative multipole interactions between electronic states involving the exchange of so called virtual photons. Both interactions are completely distinct from each other but sometimes occur simultaneously, thereby leading to the misinterpretation of physical processes. The basic difference between the two

mechanisms is that the former depends on the absolute energy of the electron in donor and acceptor states,^{15,18} whereas the later mechanism needs resonant condition of donor-acceptor electronic transitions.¹⁷ Dorenbos explained the feasibility of electron transfer processes among lanthanide ions using the vacuum referred electron binding energy (VRBE) of dopant ions.¹⁹ Accordingly, if the electron in donor state (excited state of donor ion) possesses higher energy than the acceptor state (charge transfer state of acceptor ion), the electron transfer can take place, i.e., the transfer is energetically favorable (change in free energy, ΔG^0 is negative). Figure 1 presents the VRBE diagram of lanthanide ions in borate glass.¹³ In case of Ce^{3+} , the excited $5d_1$ state is at higher energy than the Yb^{2+} ground state ($\text{Yb}^{3+} + e^-$ charge transfer), indicating that the electron transfer process is energetically favorable. Similar treatment is applicable to other dopant pairs such as Ce^{3+} - Eu^{3+} and Eu^{2+} - Yb^{3+} , where the

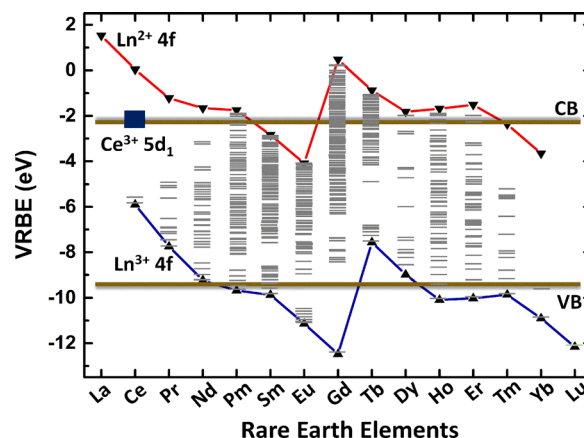


FIG. 1. VRBE scheme of di-valent and tri-valent lanthanide ions in borate glass.

^{a)}E-mail: sontakke.atul.55a@st.kyoto-u.ac.jp

donor's excited state is at higher energy than the acceptor's charge transfer state.

Several efforts have been made recently to experimentally demonstrate the electron transfer process. Setlur and Shiang adopted a semi-classical thermodynamic approach based on the Marcus theory of electron transfer.²⁰ Accordingly, the $\text{Ce}^{3+}\text{-Yb}^{3+}/\text{Eu}^{3+}$ interactions in $\text{Y}_3\text{Al}_5\text{O}_{12}$ and $\text{Lu}_2\text{Si}_2\text{O}_7$ exhibit an exponential distance dependence and a change in free energy, characteristic to the electron transfer process. In an another report, Yu *et al.* analyzed the time evolution of Ce^{3+} (donor) luminescence decay in $\text{Ce}^{3+}\text{-Yb}^{3+}$ codoped $\text{Y}_3\text{Al}_5\text{O}_{12}$ ceramic using theoretical models for electron transfer, single-photon energy transfer, and cooperative energy transfer processes.¹² They observed that the simulations show better correlation for electron transfer process over the energy transfer processes. In addition, a temperature dependence on both Ce^{3+} and Yb^{3+} luminescence behavior was observed and attributed to the thermally stimulated sensitization and quenching process.

From all these studies, it is clear that the electron transfer process exhibits temperature sensitivity. This feature can be further exploited to understand and distinguish the electron transfer process from the energy transfer processes in a more simplistic way. This has been considered in present study along with the study of luminescence behavior of donor-acceptor ions in the electron transfer and energy transfer processes. From Fig. 1, it is clear that the $\text{Ce}^{3+} \rightarrow \text{Yb}^{3+}$ interaction is governed by electron transfer process. In $\text{Ce}^{3+} \rightarrow \text{Tb}^{3+}$, the electron transfer is energetically forbidden. However, the energy level structure of $\text{Ce}^{3+}\text{-Tb}^{3+}$ is favorable for spectral resonance suggesting that the sensitization occurs due to energy transfer process. Keeping this in view, $\text{Ce}^{3+}\text{-Yb}^{3+}$ and $\text{Ce}^{3+}\text{-Tb}^{3+}$ systems have been selected as representatives for the electron transfer and energy transfer processes, and studied for their luminescence behavior, quantum yield, and temperature dependent interaction kinetics in borate glass host.

Borate glasses with base composition of 55 B_2O_3 –20 CaO –10 Al_2O_3 –15 La_2O_3 (in mol. %) were used as host for dopant ions. Ce^{3+} singly doped and $\text{Ce}^{3+}\text{-Yb}^{3+}$, $\text{Ce}^{3+}\text{-Tb}^{3+}$ codoped glasses were obtained by partially substituting the La^{3+} contents with the respective dopants. The Ce^{3+} contents were 0.5 mol. % equivalent of La_2O_3 , whereas the Yb^{3+} and Tb^{3+} contents were 1 to 3 mol. % equivalent of La_2O_3 , respectively. CeF_3 , Yb_2O_3 , and Tb_4O_7 were used as the precursor chemicals for the dopant ions, and the glasses were prepared using high temperature melt quenching method in strong reducing conditions to prevent the formation of Ce^{4+} and Tb^{4+} . The detailed synthesis procedure is available in our earlier report.¹³ The glasses are labelled according to their dopant contents.

Photoluminescence (PL) spectra of the singly and codoped glasses were recorded in the range of 380–1200 nm by pumping with a 372 nm laser diode (LD) (Nichia Co. Ltd., NDHU110APAE3) excitation. The PL signals were collected using a 90 mm focal length quartz lens, which were then dispersed using a monochromator (Nikon, G250) and recorded using a Si photodiode detector (Electro-Optical System Inc., S-025-H). All the PL spectra were calibrated using a standard halogen lamp (Labsphere, SCL-600). The PL quantum yield

was measured using a 10 in. integrating sphere (Labsphere Inc., LMS-100) attached with multi-channel CCD detectors (Ocean Optics Inc., USB2000 and USB2000+) and 372 nm LD. Signals were calibrated using a standard halogen lamp (Labsphere, SCL-600) and an auxiliary halogen lamp for absolute spectral distribution and absorption losses, respectively. Both the PL and PL quantum yield measurements were performed at room temperature. The donor (Ce^{3+}) luminescence decay measurements were carried out at varied temperatures from 15 K to 500 K using a closed-cycle He cryostat (CRT-006-2600, Iwatani), a precise temperature controlled heater and a PL lifetime measurement setup (Hamamatsu-Photonics, Quantarus Tau) equipped with picosecond LED (temporal resolution ~ 0.5 ns).

Figures 2(a) and 2(b) present the PL spectra of the studied glasses doped with $\text{Ce}^{3+}\text{-Yb}^{3+}$ and $\text{Ce}^{3+}\text{-Tb}^{3+}$ ions, respectively. In both the cases, the Ce^{3+} (donor) emission peaking at about 450 nm decreases on acceptor codoping accompanied by the appearance of acceptor's emission. In case of $\text{Ce}^{3+}\text{-Yb}^{3+}$, a weak Yb^{3+} emission is observed at about 1 μm , whereas $\text{Ce}^{3+}\text{-Tb}^{3+}$ codoped glass showed intense Tb^{3+} emissions in the visible region. A prominent difference in the studied cases is the trend in donor luminescence quenching and sensitized acceptor emission intensity. The donor (Ce^{3+}) emission undergoes more quenching in $\text{Ce}^{3+}\text{-Yb}^{3+}$ codoped glass over the $\text{Ce}^{3+}\text{-Tb}^{3+}$ codoped glass, however the sensitized luminescence is significantly weak in former case compared to the later one.

This difference is due to the different nature of donor-acceptor interactions, i.e., electron transfer and energy transfer processes. The electron transfer process in $\text{Ce}^{3+}\text{-Yb}^{3+}$ pair is relatively more stronger compared to the energy transfer process in $\text{Ce}^{3+}\text{-Tb}^{3+}$, thereby giving rise to larger quenching of donor excitation.²⁰ On the contrary, the donor's energy is directly utilized in the excitation of acceptor ion in energy transfer process; but in case of electron transfer process, it may or may not excite the acceptor ion.^{13–15} This incorporates an additional parameter defining the probability of acceptor excitation per electron transfer interaction (P_A^*). As in energy transfer process, the sensitized luminescence

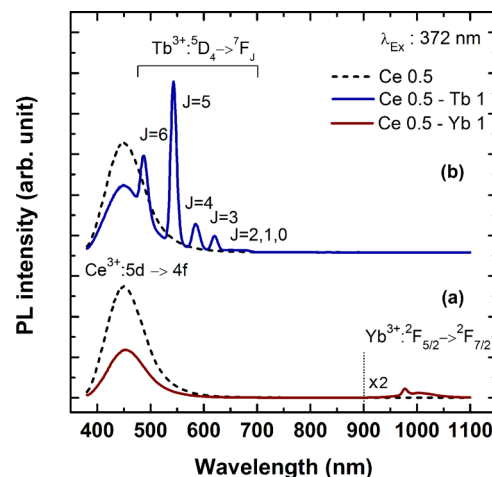


FIG. 2. PL spectra of donor singly doped (dotted line) and donor-acceptor codoped (solid line) samples exhibiting (a) $\text{Ce}^{3+}\text{-Yb}^{3+}$ and (b) $\text{Ce}^{3+}\text{-Tb}^{3+}$ ions.

mainly depends on the donor-acceptor interaction efficiency and the acceptor's quantum efficiency; it is also accompanied by P_A^* parameter in the electron transfer process, which plays a vital role in determining the sensitized luminescence intensity. The literature reports reveal that the sensitized luminescence intensity is usually poor in electron transfer process.^{12–15} Also, it exhibits a temperature dependence as has been observed by Yu *et al.* in $\text{Ce}^{3+}\text{-Yb}^{3+}$: $\text{Y}_3\text{Al}_5\text{O}_{12}$ giving rise to a decrease in Yb^{3+} luminescence at room temperature.¹² This was attributed to be due to the thermally activated intersystem crossing of $\text{Ce}^{4+}\text{-Yb}^{2+}$ charge transfer state to the Yb^{3+} ground state at elevated temperature ($T > 120\text{ K}$). Interestingly, a similar experiment on present $\text{Ce}^{3+}\text{-Yb}^{3+}$ codoped glasses suggested a small increase in the sensitized Yb^{3+} luminescence with increase in temperature above 100 K. The exact nature of sensitization mechanism in electron transfer process is still not clear and requires an independent detailed study. However, the experimental evidence clearly suggests that the probability of acceptor excitation (P_A^*) is very low and is responsible for the poor sensitized luminescence intensity even if the donor-acceptor interactions are superior in electron transfer process.

This has also been reflected in the luminescence quantum yield of studied glasses obtained from integrating sphere experiment.²¹ For Ce^{3+} singly doped glass, the experimental quantum yield is 41.6%. It exhibits a sharp decline to 16.1% in $\text{Ce}^{3+}\text{-Yb}^{3+}$ glass, whereas in $\text{Ce}^{3+}\text{-Tb}^{3+}$ glass, it increases slightly to 42.5%. This is consistent with the PL characteristics. The electron transfer process in $\text{Ce}^{3+}\text{-Yb}^{3+}$ strongly quenches the Ce^{3+} luminescence, but it does not lead to an efficient acceptor sensitization. However, in case of $\text{Ce}^{3+}\text{-Tb}^{3+}$, each de-excited Ce^{3+} ion populates one Tb^{3+} ion. Interestingly, the quantum yield shows a slight increase in $\text{Ce}^{3+}\text{-Tb}^{3+}$ codoped glass over the Ce^{3+} singly doped glass. Although the increase is within the experimental uncertainty, there may also be some genuine reasons including the reduced contribution of Ce^{3+} thermal ionization due to the energy transfer to Tb^{3+} in codoped glass as well as the occurrence of Tb^{3+} self-excited luminescence under 372 nm excitation.

To get more insight of the electron transfer and energy transfer processes, the donor luminescence decay kinetics have been studied as a function of temperature. Figure 3(a) shows the Ce^{3+} decay lifetime in singly and codoped glasses in the temperature range of 15 K to 500 K. The decay lifetime has been obtained by fitting the decay profiles with exponential decay functions.^{14,22} In case of Ce^{3+} singly doped glass, the decay profiles were nearly single exponential at low temperature range. However, it became non-exponential at higher temperature and in the codoped glasses. The second order exponential decay function was used to obtain the average decay lifetime for non-exponential decay profiles.²² The decay lifetime is about 51 ns in Ce^{3+} singly doped glass at low temperature and exhibits a decrease above about 100 K. This decrease in decay lifetime with temperature is due to the thermal activation of Ce^{3+} $5d_1$ excited state electrons to the conduction band as represented in Fig. 4(a).¹³ The proximity of $5d_1$ excited state of Ce^{3+} to the bottom of the conduction band (Fig. 1) results in the ionization of

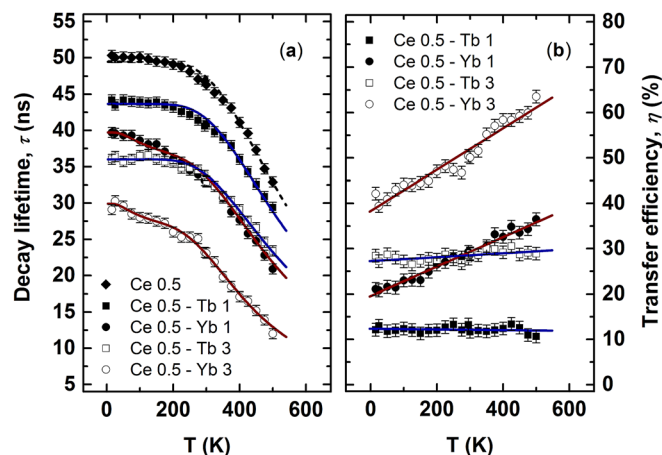


FIG. 3. Temperature dependence on donor luminescence decay lifetimes (a), and transfer efficiency (b). The fits to the experimental data represents theoretical simulations.

excitation population at elevated temperatures. The activation energy for thermal ionization has been obtained from the theoretical fit to the experimental data simulated using Arrhenius relation as given below^{23,24}

$$\tau_{Ce}^{-1} = A_0 + A_1 \exp\left(\frac{-E_a}{k_B T}\right), \quad (1)$$

where τ_{Ce} is the Ce^{3+} $5d_1 \rightarrow 4f$ decay lifetime, A_0 and A_1 are constants representing intrinsic radiative decay rate and the attempt rate for thermal ionization process, respectively, k_B is Boltzmann constant, T is absolute temperature, and E_a is the activation energy for thermal ionization. From the fit, E_a is obtained to be $135 \pm 10\text{ meV}$ and A_1 is about $3.90 \pm 0.01 \times 10^8\text{ s}^{-1}$.

In $\text{Ce}^{3+}\text{-Tb}^{3+}$ glass, the decay lifetime exhibits an overall decrease due to the $\text{Ce}^{3+} \rightarrow \text{Tb}^{3+}$ energy transfer. However, the trend of decay lifetime with temperature is similar to that of Ce^{3+} singly doped glass. A further decrease in decay lifetime is observed in case of $\text{Ce}^{3+}\text{-Yb}^{3+}$ glass, which is consistent with the PL studies revealing relatively more quenching of donor excitation. Moreover, the trend of decay lifetime with temperature does not coincide with the former cases. The decay lifetime exhibits faster decrease with temperature in $\text{Ce}^{3+}\text{-Yb}^{3+}$ codoped glass compared to the Ce^{3+} singly doped and $\text{Ce}^{3+}\text{-Tb}^{3+}$ codoped glasses. This directly substantiates the presence of an additional temperature

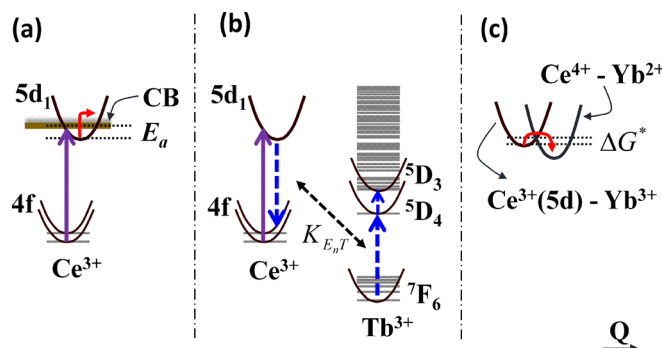


FIG. 4. Schematic illustration of (a) thermal ionization, (b) energy transfer, and (c) electron transfer process (figure not in scale).

dependent process. By considering the interaction mechanisms involved, the data have been fitted with theoretical simulations based on the following relations:

$$\tau_{Ce-Tb}^{-1} = A_0 + A_1 \exp\left(\frac{-E_a}{k_B T}\right) + K_{E_n T}, \quad (2)$$

$$\tau_{Ce-Yb}^{-1} = A_0 + A_1^* \exp\left(\frac{-E_a}{k_B T}\right) + B_0 + B_1 \exp\left(\frac{-\Delta G^*}{k_B T}\right), \quad (3)$$

where $K_{E_n T}$ is the energy transfer rate, B_0 and B_1 are the temperature independent reaction rate and frequency factor for thermally stimulated electron transfer respectively, and ΔG^* is the Gibbs free energy for the formation of transition state for electron transfer interactions (Marcus theory).^{23,25} The additional terms on the right hand side of Eqs. (2) and (3) represent the contribution of energy transfer and electron transfer processes as can be understood from the Figs. 4(b) and 4(c), respectively. The $Ce^{3+} \rightarrow Tb^{3+}$ energy transfer rate, $K_{E_n T}$, is obtained to be $2.68 \pm 0.01 \times 10^6 s^{-1}$ for Ce05-Tb1 glass and is almost constant in the studied temperature range. Basically, the energy transfer rate (resonant case) is a function of donor-acceptor distance and the oscillator strengths of the interacting transitions.^{17,26} It does not specifically need thermal activation and therefore is temperature independent, provided the oscillator strengths remain unperturbed and phonon contribution (non-resonant case) is minimum. However, the electron transfer process involves the physical displacement of electron through an intermediate transition state with an activation energy ΔG^* . From the fit, ΔG^* is obtained to be 11 ± 2 meV. This indicates that an electron needs to overcome about 11 meV potential barrier in Ce^{3+} - Yb^{3+} electron transfer process and therefore, the interaction becomes more efficient with the increase in temperature. Note that ΔG^* is very small compared to E_a . The competing reaction rate of electron transfer process can possibly affect the ionization probability of Ce^{3+} ions to the conduction band in Ce^{3+} - Yb^{3+} codoped glass ($A_1^* = 4.50 \pm 0.01 \times 10^8 s^{-1}$). Moreover, the electron transfer process accompanies a temperature independent parameter B_0 , which is also believed to be present in other such cases, like Ce^{3+} - Yb^{3+} : $Y_3Al_5O_{12}$ ceramics.^{12,15} The origin of this parameter may be due to the Ce^{3+} - Yb^{3+} pairs, where the interactions deviate from the classical Marcus approach and exhibits more quantum like behavior, i.e., quantum tunneling.²⁷ However, more detail study is required to substantiate it. From the fit, the B_0 and B_1 are obtained to be $4.95 \pm 0.01 \times 10^6 s^{-1}$ and $4.20 \pm 0.01 \times 10^6 s^{-1}$, respectively, for Ce05-Yb1 glass.

Figure 3 also presents the temperature dependence of Ce^{3+} decay lifetime for glasses exhibiting higher acceptor concentrations (3 mol%). Note that the trend in decay lifetime with temperature is similar in both acceptor concentrations. The theoretical fits revealed an increased $K_{E_n T}$ ($7.55 \pm 0.01 \times 10^6 s^{-1}$) in Ce05-Tb3 glass and B_0 ($1.32 \pm 0.01 \times 10^7 s^{-1}$) in Ce05-Yb3 glass, which is expected due to the shortening of donor-acceptor separation. The A_1^* and B_1 is $6.63 \pm 0.01 \times 10^8 s^{-1}$ and $6.50 \pm 0.01 \times 10^6 s^{-1}$ in Ce05-Yb3 glass. The intrinsic decay rate (A_0), attempt rate (A_1), activation energy for thermal ionization (E_a), and electron transfer (ΔG^*) are constant throughout the fittings.

Figure 3(b) shows the temperature dependence of the donor to acceptor electron/energy transfer efficiency. The transfer efficiency (η) has been calculated from the donor decay lifetime for singly (τ_{Ce}) and codoped ($\tau_{Ce-Tb/Yb}$) glasses using the following relation:¹⁴

$$\eta = 1 - \frac{\tau_{Ce-Tb/Yb}}{\tau_{Ce}}. \quad (4)$$

The results reveal a steady increase in transfer efficiency for Ce^{3+} - Yb^{3+} electron transfer process with the increase in temperature. In Ce^{3+} - Tb^{3+} energy transfer, the transfer efficiency is nearly constant in the studied temperature range. This substantiates that the temperature dependent transfer efficiency could be an effective feature to identify and differentiate the electron transfer process from the energy transfer processes.

Similar to decay lifetime, the temperature dependent steady state luminescence also provides compatible information and can be used as an alternative method to discriminate the donor-acceptor interactions. However, the decay lifetime is more absolute and reliable over steady state luminescence for quantitative analysis.²⁸ The steady state luminescence is highly sensitive to temperature induced changes in the absorption strengths as well as other physical parameters.²⁸ On the contrary, the intrinsic decay lifetime (A_0^{-1}) for allowed transitions does not exhibit significant variation with the temperature.²⁹

In conclusion, temperature dependent donor decay kinetics is shown to be an effective tool to describe the donor-acceptor interaction mechanism between rare earth lanthanide ions. The interaction efficiency showed a steady rise with temperature for $Ce^{3+} \rightarrow Yb^{3+}$ electron transfer process; however, it remained nearly constant for the $Ce^{3+} \rightarrow Tb^{3+}$ energy transfer process. This behavior has been explained due to the presence of electron transfer transition state requiring thermal activation. A quantitative analysis of reaction parameters has been proposed using the rate equation modeling. In addition, the consequences of electron transfer and energy transfer processes on luminescence properties, quantum yield, and decay lifetime have been presented and discussed. The results in this study will help to further extend the present understanding of donor-acceptor interaction dynamics among lanthanide ions in dielectric hosts.

This work was carried out under the JSPS post-doctoral fellowship program (P13372) and also supported by JST-PRESTO.

¹J. M. Maijer, L. Aarts, B. M. van der Ende, T. J. H. Vligt, and A. Meijerink, *Phys. Rev. B* **81**, 035107 (2010).

²D. Serrano, A. Braud, J. L. Doualan, W. Bolaños, R. Moncorgé, and P. Camy, *Phys. Rev. B* **88**, 205144 (2013).

³J. L. Sommerdijk, A. Bril, and A. W. de Jager, *J. Lumin.* **8**, 341 (1977).

⁴B. M. van der Ende, L. Aarts, and A. Meijerink, *Phys. Chem. Chem. Phys.* **11**, 11081 (2009).

⁵R. T. Wegh, H. Donker, K. D. Oskam, and A. Meijerink, *Science* **283**, 663 (1999).

⁶F. Auzel, *Chem. Rev.* **104**, 139 (2004).

⁷L. Aarts, B. M. van der Ende, and A. Meijerink, *J. Appl. Phys.* **106**, 023522 (2009).

- ⁸A. Boccolini, J. Marques-Hueso, D. Chen, Y. Wang, and B. S. Richards, *Sol. Energy Mater. Sol. Cells* **122**, 8 (2014).
- ⁹Z. Liu, J. Li, L. Yang, Q. Chen, Y. Chu, and N. Dai, *Sol. Energy Mater. Sol. Cells* **122**, 46 (2014).
- ¹⁰P. Song and C. Jiang, *IEEE Photonics J.* **5**, 8400110 (2014).
- ¹¹J. Zhou, Y. Zhuang, S. Ye, Y. Teng, G. Lin, B. Zhu, J. Xie, and J. Qiu, *Appl. Phys. Lett.* **95**, 141101 (2009).
- ¹²D. C. Yu, F. T. Rabouw, W. Q. Boon, T. Kieboom, S. Ye, Q. Y. Zhang, and A. Meijerink, *Phys. Rev. B* **90**, 165126 (2014).
- ¹³A. D. Sontakke, J. Ueda, Y. Katayama, Y. Zhuang, P. Dorenbos, and S. Tanabe, *J. Appl. Phys.* **117**, 013105 (2015).
- ¹⁴J. Ueda and S. Tanabe, *J. Appl. Phys.* **106**, 043101 (2009).
- ¹⁵F. You, A. J. J. Bos, Q. Shi, S. Huang, and P. Dorenbos, *J. Phys.: Condens. Matter* **23**, 215502 (2011).
- ¹⁶R. Huber, *Angew. Chem. Int. Ed.* **28**, 848 (1989).
- ¹⁷R. C. Powel, *Physics of Solid State Laser Materials* (Springer-Verlag, New York, 1998).
- ¹⁸P. Dorenbos, A. J. J. Bos, and N. R. J. Poolton, *Phys. Rev. B* **82**, 195127 (2010).
- ¹⁹P. Dorenbos, *J. Mater. Chem.* **22**, 22344 (2012).
- ²⁰A. A. Setlur and J. J. Shiang, *J. Phys. Chem. C* **114**, 2792 (2010).
- ²¹J. C. de Mello, H. F. Wittmann, and R. H. Friend, *Adv. Mater.* **9**, 230 (1997).
- ²²T. Fujii, K. Kodaira, O. Kawauchi, and N. Tanaka, *J. Phys. Chem. B* **101**, 10631 (1997).
- ²³P. L. Houston, *Chemical Kinetics and Reaction Dynamics* (McGraw-Hill, New York 2001).
- ²⁴J. Ueda and S. Tanabe, *J. Appl. Phys.* **110**, 053102 (2011).
- ²⁵R. A. Marcus and N. Sutin, *Biochim. Biophys. Acta* **811**, 265 (1985).
- ²⁶A. D. Sontakke and K. Annapurna, *J. Appl. Phys.* **112**, 013510 (2012).
- ²⁷A. Lecointre, A. Bessière, A. J. J. Bos, P. Dorenbos, B. Viana, and S. Jacquart, *J. Phys. Chem. C* **115**, 4217 (2011).
- ²⁸J. M. Ogiegło, A. Katelnikovas, A. Zych, T. Jüstel, A. Meijerink, and C. R. Ronda, *J. Phys. Chem. A* **117**, 2479 (2013).
- ²⁹V. Bachmann, C. Ronda, and A. Meijerink, *Chem. Mater.* **21**, 2077 (2009).